A rate and pressure dependent elastoplastic material model for glacial ice colliding with marine structures

M. Mokhtari, E. Kim & J. Amdahl
Centre for Autonomous Marine Operations and Systems (AMOS), Department of Marine Technology, Norwegian University of Science and Technology (NTNU), Norway

ABSTRACT: An elastoplastic ice material model with a rate and pressure dependent yield criterion is proposed in the present study for ice-structure collision simulations. The yield criterion is based upon the Tsai-Wu failure envelope which is formulated in the present study to evolve with the strain rate. The relation between ice strength and loading rate is known to be disrupted at the 'ductile-to-brittle transition' strain rate. Hence, the yield locus evolves differently in ductile and brittle regimes, which is herein modelled using two different strain rate-strength equations. These equations, obtained from the literature, are based on more than 100 physical tests on freshwater polycrystalline ice, including iceberg ice samples. The constitutive laws, written in Fortran, are implemented in Abaqus as vectorised user material (VUMAT). The proposed material model is validated against two physical ice crushing tests with different indentation speeds, 1 mm/s and 100 mm/s.

1 INTRODUCTION

Marine structures in the icy waters must withstand the impact loads induced by floating ice features. However, design against ice impact in marine engineering applications is still challenging due to the uncertainties associated with the varied compositional and microstructural properties of ice, as well as the phase transition and microstructural transformations in different loading conditions. Numerical methods, including Finite Element Methods (FEM) in particular, are extensively used to simulate and study the structural and dynamic behaviour of marine/offshore structures subject to ice impact. The accuracy of such simulations is highly dependent on the ice material model. However, there is no universal or widely accepted ice material model due to the complex and rather stochastic mechanical behaviour of ice.

Although several studies have reported viscoelastic behaviour for ice under compressive loading (Jordaan et al. 1999, Jordaan 2001, O'Rourke et al. 2016, Sinha 1978a, b, 1983, Sinha 1988, Taylor 2010, Xiao and Jordaan 1996, Xiao 1997), the most common practice employs plastic rheology to model the inelastic deformations of ice in ice-structure collision simulations (Cammaert et al. 1983, Cao et al. 2016, Gagnon and Derradji-Aouat 2006, Gagnon 2007, 2010, 2011, Gagnon and Wang 2012, Han et al. 2017, Kim and Kedward 1999, Kim and Kedward 2000, Kim 2015, Kim et al. 2015, Kim and Quinton 2016, Kim and Kim 2019, Liu et al. 2011, Obisesan and Sriramula 2018, Price et al. 2021, Schulson 2001, Wang et al. 2008).

Crushable foam (Deshpande and Fleck 2000), Drucker-Prager (1952), Mohr-Coulomb and a Tsai-Wu yield surface-based material model proposed by Liu et al. (2011) are the plasticity models that are commonly employed for ice behaviour simulations in the ice-structure collision simulations in marine applications. Among these, the model proposed by Liu et al. is the only one that has been specifically developed for ice materials. The crushable foam model was originally developed for metallic foams (Deshpande and Fleck 2000), Drucker-Prager model deals with plastic deformation of soils (Drucker and Prager 1952), and Mohr-Coulomb model is usually utilized to simulate rock, soil, concrete, and other similar geomaterials (Bai and Wierzbicki 2010). Nevertheless, these models (i.e., crushable foam, Drucker-Prager, and Mohr-Coulomb) have been employed in several studies to simulate the crushing ice behaviour since they are among the very few material models readily available in commercial software that in theory could approximate the pressure-dependent crushing ice behaviour.

Han et al. (Han et al. 2017) showed that the crushable foam model is in general more suited to model the ice-crushing process as opposed to Drucker-Prager and Mohr-Coulomb models. Mokhtari et al. (2022) compared the crushable foam model with the model proposed by Li et al. in a systemic study and found that the crushable foam model cannot simulate the confining pressure in crushing ice. On the other

hand, the model proposed by Liu et al. could capture the confining pressure and thus returned good agreements with the physical test data.

Despite the good performance of the model proposed by Liu et al., it is still rate independent. Consequently, it requires recalibration for different collision velocities because ice mechanical behaviour is rate-dependent, especially at lower loading rates. Therefore, this elastoplastic material model is modified in the present study by developing a rate and pressure dependent yield criterion incorporated in the constitutive laws to account for the loading rate effects.

2 METHODOLOGY

2.1 *Constitutive model*

To simulate the ice-crushing behaviour using Abaqus explicit solver (Dassault Systèmes SIMULIA User Assistance, Abaqus 2019), a vectorised user material (VUMAT) was written in Fortran. The VUMAT was developed based on the constitutive model presented in this section.

The yield strength of ice is demonstrated to be a pressure and rate dependent property (Derradji-Aouat 2000, Derradji-Aouat and Evgin 2001, Derradji-Aouat 2003, Derradji-Aouat 2005, Derradji-Aouat et al. 2015, Golding et al. 2010, Gratz and Schulson 1997, Iliescu and Schulson 2004, Sain and Narasimhan 2011, Sammonds et al. 1998, Schulson 1990, Schulson and Gratz 1999, Timco and Frederking 1986, Weiss and Schulson 1995). Based on experimental data obtained from triaxial testing of around 300 isotropic ice samples under a wide range of strain rates ($10^{-6} < \dot{\varepsilon} < 10^{-1}$ s^{-1}) and hydrostatic pressures (0.1 < p < 85.0 MPa), Derradji-Aouat (Derradji-Aouat 2000) reported that the failure/yield stress data plotted in p-τ_{oct} space follow an elliptical curve. The octahedral shear stress, τ_{oct}, is defined by

$$\tau_{oct} = \sqrt{\frac{s_{ij}s_{ij}}{3}} \tag{1}$$

where s_{ij} denotes a component in the deviatoric stress tensor. Accordingly, an elliptical yield surface based on the Tsai-Wu yield criterion (Tsai and Wu 1971) can be expressed for isotropic ice by

$$(\frac{\tau_{oct}-\eta}{\tau_{max}})^2+(\frac{p-\xi}{p_c})^2=1 \tag{2}$$

where η, τ_{max}, ξ, and p_c are constants ($\eta = 0$). Equation (2) can be rewritten in the p-s space as

$$\Phi \equiv \varphi(p,s)=\sqrt{s^2+\alpha^2(p-p_0)^2}-B=0 \tag{3}$$

where $\Phi \equiv \varphi(p,s)$ is the yield surface or the plastic potential function (associated flow rule); s is the von Mises stress; $B = \alpha A = \alpha(\frac{p_c+p_t}{2})$ determines the ellipse vertical semiaxis (along the s-axis in Figure 1a); $\alpha = \frac{B}{A}$ denotes the shape factor determining the relative magnitude of the semiaxes; A is the ellipse horizontal semiaxis (along the p-axis); $p_0 = \frac{p_c-p_t}{2}$ is the ellipse centre on the p-axis found from p_t and p_c which respectively are the ice material strength under hydrostatic tension and hydrostatic compression (p_c is always positive). α is related to the yield stress in uniaxial compression, σ_c, failure strength in hydrostatic compression, p_c, and the failure strength in hydrostatic tension, p_t, by

$$\alpha = \frac{3k}{\sqrt{(3k_t+k)(3-k)}} \; ; \; k = \frac{\sigma_c}{p_c} \; ; \; k_t = \frac{p_t}{p_c} \tag{4}$$

provided that

$$0 < k < 3 \;\; \& \;\; k_t \geq 0 \tag{5}$$

While B increases with the strain rate in ice (except for the ductile-to-brittle transition phase), p_t and p_c are known to be insensitive to strain rate (Derradji-Aouat 2000, Derradji-Aouat and Evgin 2001, Derradji-Aouat 2005, Derradji-Aouat et al. 2015). As such, for a set of strain rates, a set of concentric elliptical yield loci exist (Figure 1b). In triaxial compressive testing of ice specimens, the strain rate hardening of ice is disrupted at a certain range of strain rates. This is known as the 'ductile-to-brittle transition' strain rate. The transition strain rate is reported to be between 10^{-4} and 10^{-2} s^{-1} in different studies (Cai et al. 2020, Gagnon and Gammon 1995, Gupta and Bergström 2002, Ince, Kumar and Paik 2017, Ince, Kumar, Park, et al. 2017, Jones 2007, Michel and Toussaint 1977, Schulson 2001, Snyder et al. 2016). In the transition phase, ice yield strength remains unchanged or slightly decreases and then continues to rise in the brittle regime, but with a rate less than in the ductile regime (Figure 1c). This behaviour of ice is reflected in the constitutive model using Jones' relation (Jones 2007) for the ductile regime ($\dot{\varepsilon} \leq 0.001$ in Equation (6)) and Shazly et al. equation (Shazly et al. 2009) for the brittle regime ($\dot{\varepsilon} > 0.001$ in Equation (6)). These equations are based on more than 100 physical tests on freshwater polycrystalline ice, including iceberg ice samples.
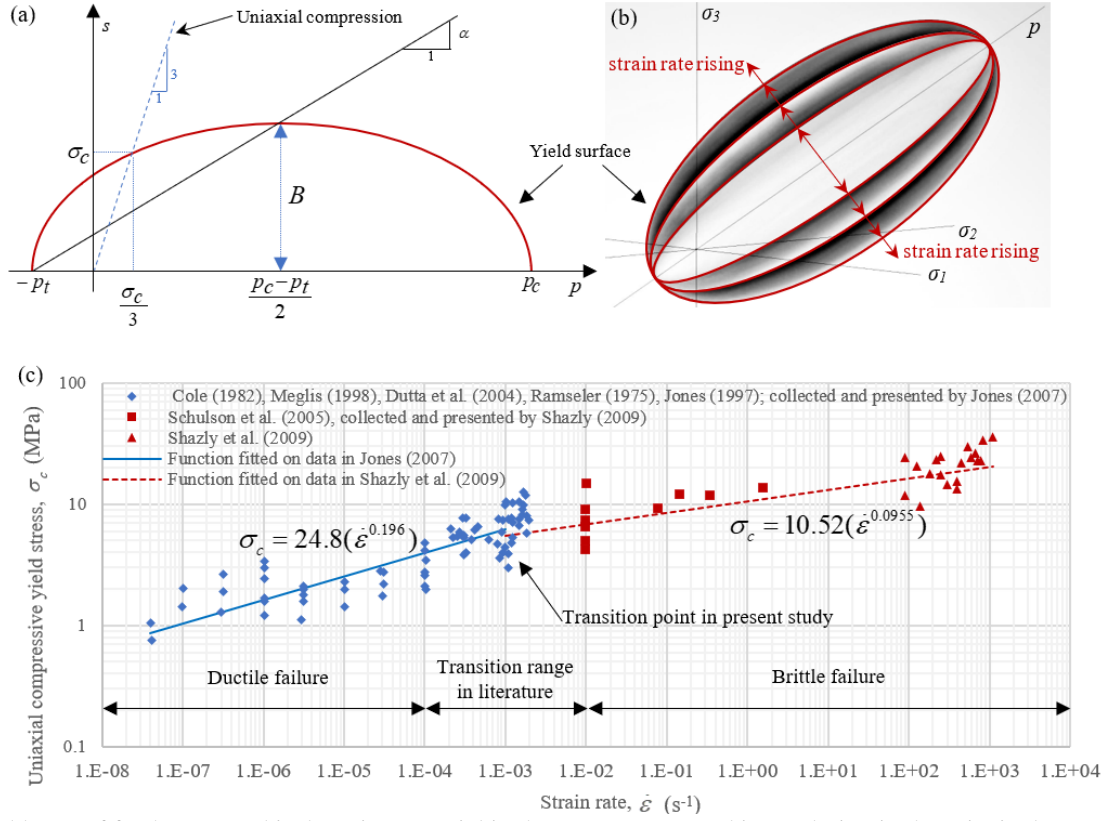
Figure 1. Yield locus of freshwater and iceberg ice material in the *p-s* space (a) and its evolution in the principal stress space (σ_1-σ_2-σ_3) (b), which is governed by the strain rate hardening formulation plotted in (c).

$$\sigma_c = \begin{cases} 24.8(\dot{\varepsilon}^{0.196}) & \text{if } \dot{\varepsilon} \leq 0.001 \\ 10.52(\dot{\varepsilon}^{0.0955}) & \text{if } \dot{\varepsilon} > 0.001 \end{cases} \qquad (6)$$

With σ_c obtained from Equation (6), the yield stress, s_y, for given pressures and strain rates can be found from Equation (3). The trial stresses exceeding the yield stress, s_y, are mapped back on the yield surface using the Cutting Plane Algorithm (CPA), and the strains are updated accordingly. The mathematical framework for stress-strain correction using CPA is thoroughly explained in (Mokhtari et al. 2022).

To determine the failure of the ice material, a general form (Equation (7)) of the failure model proposed by Liu et al. (2011) is employed.

$$\varepsilon_f = \varepsilon_0 + \left(\frac{p}{M\,p_c} - \frac{N}{M} \right)^2 \qquad (7)$$

where ε_f is the failure strain while ε_0 is the reference/initial failure strain and M and N are constants. If the equivalent plastic strain, $\bar{\varepsilon}^p$, exceeds the failure strain in an element (i.e., $\bar{\varepsilon}^p > \varepsilon_f$), erosion is activated, and the element is disregarded in the rest of the analysis. The equivalent plastic strain can be described by

$$\bar{\varepsilon}^p = \sqrt{\frac{2}{3}\mathbf{e}^p : \mathbf{e}^p} \qquad (8)$$

where $\mathbf{e}^p$ is the deviatoric plastic strain tensor. Note that the nodes of eroded elements become free-flying point masses that could transfer momentum to the active contact faces (Dassault Systèmes SIMULIA User Assistance, Abaqus 2019).

2.2 Finite element modelling

To validate the constitutive model presented in the present study, two ice-crushing tests carried out by Kim et al. (Kim et al. 2015) are simulated. These tests use flat rigid indenters (Figure 2) moving with two different speeds of 100 and 1 mm/s. The first test with V=100 mm/s better represents the loading rates in collision scenarios. However, the second test was simulated to investigate the rate sensitivity of the constitutive model.

Considering the geometrical and load symmetries, a quarter finite element model of the conical ice sample is developed (Figure 2) for computational efficiency. Note a sensitivity study with both a quarter model and a full model was first carried out to ensure the quarter and full models produce very similar results. The model is discretised into 76344 linear hexahedral elements with reduced integration (C3D8R) based on the mesh sensitivity analysis presented in (Mokhtari et al. 2022).

The uniform mesh in Figure 2 was generated through a manual, incremental meshing process, known as 'bottom-up meshing'. This uniformly meshed model ensures more efficient and accurate simulations as opposed to automatically meshed models. The automatic meshing of the conical geometry produces elements with significantly different sizes, shapes and aspect ratios, not desirable for testing the constitutive model. Besides, the automatic meshing could generate poor-quality elements that significantly slow down the processing or cause its failure due to large element distortions. The boundary conditions imposed by the ice holder are illustrated in Figure 2.

A list of input parameters for the material model is provided in Table 1. Young's modulus, E, elastic Poisson's ratio, v_e, and the initial density, ρ_0, were obtained from (Liu et al. 2011); p_c and p_t for the plasticity model were taken from (Derradji-Aouat 2000). With these input parameters, M and N were found from a calibration study.
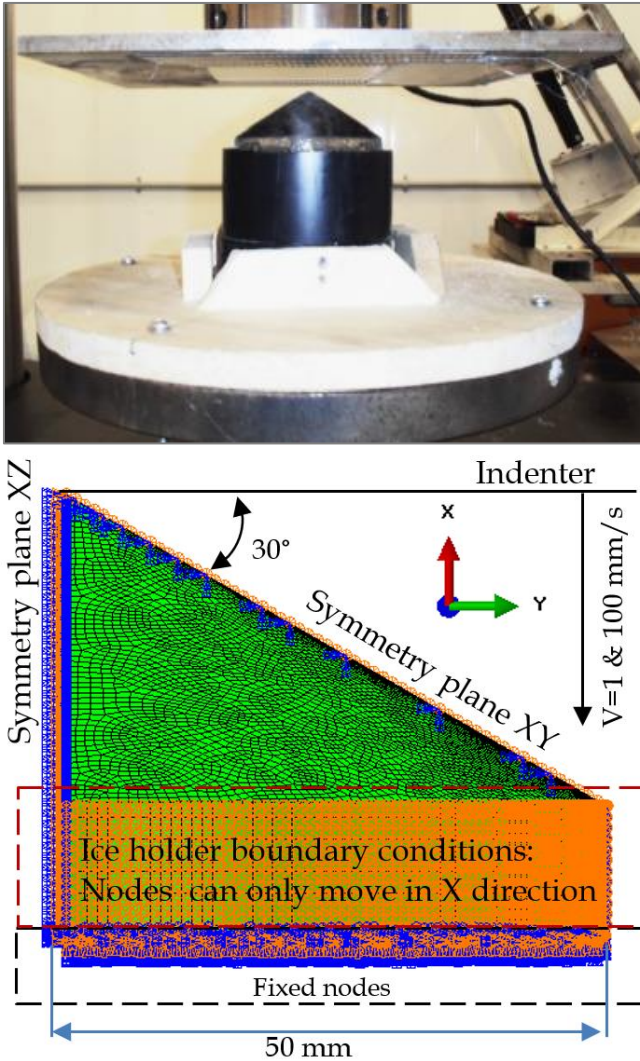
Figure 2. Conical ice sample for crushing tests in the experimental study (Kim et al. 2015) (a) and the finite element simulation (b).

Table 1. Material parameters of the proposed model for the conical ice sample in the present study.

E (MPa)	v_e	ρ_0 (kg/m³)	p_c (MPa)	p_t (MPa)	M	N
9500	0.3	900	100.0	10.0	1.0	0.5

3 RESLUTS, VALIDATION AND DISCUSSION

The experimental and numerical force-displacement, F-D, curves are compared in Figure 3, where F is the normal force due to the contact pressure and is a function of indenter speed, V, and displacement, D (i.e., $F \equiv f(V,D)$). At two points in Figure 3, the experimental forces fall abruptly which is due to pausing the indentation for data collection (Kim et al. 2015). The tests were resumed after the data collection. These interruptions are not simulated in the present study. Disregarding these discontinuities in the experimental curves, the numerical results produced by the proposed model correlate closely with the experimental data for both indentations speeds.

Figure 3 shows regular oscillation in the numerical reaction forces superimposed with very high-frequency noise. High-frequency noise is typical in explicit collision simulations (Dassault Systèmes SIMULIA User Assistance, Abaqus 2019) while the force oscillation is due to element erosion. Consequently, the frequency and amplitude of the force oscillation largely depend on the element size. However, the mean reaction force is unlikely to be much sensitive to the element size when the proposed model is applied according to a mesh sensitivity analysis by (Mokhtari et al. 2022).

In Figure 3, the experimental reaction force from the 1 mm/s test is relatively smaller than that from the 100 mm/s test, which is replicated by the proposed model. To more closely evaluate the influence of indentation speed on the reaction force, noise-filtered numerical F-D curves are compared relative to each other in Figure 4. Note that the noise/oscillation was removed using Butterworth filter (Dassault Systèmes SIMULIA User Assistance, Abaqus 2019) with a cutoff frequency of 0.5 Hz. The relative difference between the reaction forces is also plotted in Figure 4, which was calculated by

$$R \equiv r(V, V_0, D) = \frac{f(V,D) - f(V_0,D)}{f(V_0,D)} \qquad (9)$$

where R is the relative difference as a function of D, V, and the reference indentation speed, V_0, which is 1 mm/s in the present study. In Figure 4, R fluctuates significantly until $D \approx 11$ mm, and then stabilizes. After the stabilization, R fluctuates between 10.5% and 13.4%.

The improvement made to the original model by adding the strain rate dependency formulation to it is obvious when Figure 4 is compared with Figure 5. In Figure 5, the noise-filtered numerical F-D curves obtained from the original, rate-independent model are presented. The yield surface in the original material model is fixed and σ_c must be provided to the model as a single scalar value. With σ_c set to 22.8 MPa and

without changing the other material parameters, the original model produced almost the same F-*D* curve for the 100 mm/s study as the modified model. However, it was not able to capture the reaction force drop caused by the slower loading rate in the 1 mm/s study such that R in Figure 5 fluctuates around just 4.3% after *D*≈11 mm. Note that this was around 12% for the results produced by the modified material model (Figure 4).
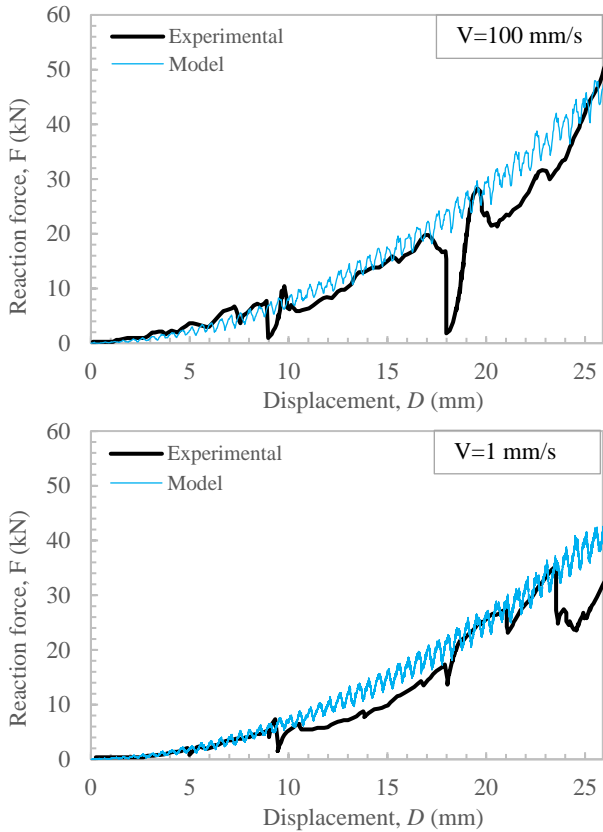
Figure 3. Force vs. displacement from the experimental study (Kim et al. 2015) and the modified (rate-dependent) material model presented in this study.
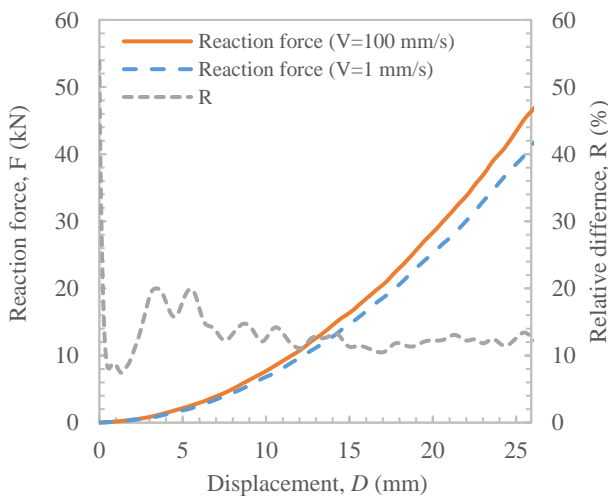
Figure 4. Numerical *F-D* curves by the modified (rate-dependent) material model after noise removal using Butterworth filter and their relative difference, R.
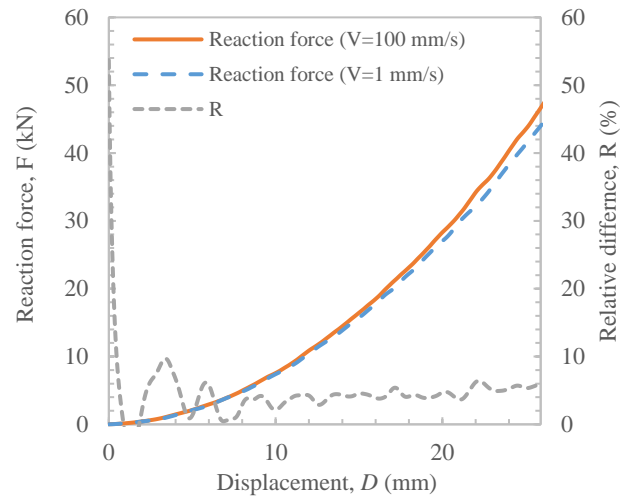
Figure 5. Numerical *F-D* curves by the original (rate-independent) material model after noise removal using Butterworth filter and their relative difference, R.

4 CONCLUSIONS

A rate and pressure dependent yield criterion is proposed in the present study to improve the elastoplastic modelling of the ice-crushing process in ice-structure collision simulations. The yield criterion is based on the Tsai-Wu yield surface which is herein formulated to evolve with the strain rate. The strain rate-strength data is obtained from the literature and is based on more than 100 physical tests on freshwater polycrystalline ice, including iceberg ice samples. These tests covered a wide range of strain rates ($\sim 10^{-8} < \dot{\varepsilon} < \sim 10^{3}$ s^{-1}) in both ductile and brittle regimes. Combined with a general form of the failure model of Liu et al., the proposed model was written in Fortran. Then, it was implemented in Abaqus/Explicit finite element code to simulate two physical ice crushing tests on conical ice samples with different indentation speeds, 1 and 100 mm/s.

Comparative analyses of the numerical and experimental results demonstrated that the proposed model can replicate the loading rate effect on the reaction force. The numerical reaction force was dropped by around 12% on average when the indention speed was reduced from 100 mm/s to 1 mm/s. Overall, the numerical results in terms of force-displacement simulated using the proposed model correlated closely with the experimental data.

5 REFERNCES

Bai Y, Wierzbicki T (2010) Application of extended Mohr–Coulomb criterion to ductile fracture. International journal of fracture 161(1):1-20.

Cai W, Zhu L, Yu TX, Li Y (2020) Numerical simulations for plates under ice impact based on a concrete constitutive ice model. International Journal of Impact Engineering 143:103594.

Cammaert A, Wong T, Curtis D (1983) Impact of icebergs on offshore gravity and floating platforms.

Cao B, Bae DM, Sohn JM, Prabowo AR, Chen TH, Li H (2016) Numerical analysis for damage characteristics caused by ice collision on side structure. International Conference on Offshore Mechanics and Arctic Engineering.

Dassault Systèmes SIMULIA User Assistance, Abaqus. (2019).

Derradji-Aouat A (2000) A unified failure envelope for isotropic fresh water ice and iceberg ice. Proceedings of ETCE/OMAE Joint Conference Energy for the New Millenium.

Derradji-Aouat A, Evgin E (2001) Progressive damage mechanism for ductile failure for polycrystalline ice and its complementary brittle failure criterion. OMAE-2001, Rio de Janeiro, Brazil Polar and Arctic session 6002.

Derradji-Aouat A (2003) Multi-surface failure criterion for saline ice in the brittle regime. Cold Regions Science and Technology 36(1):47-70.

Derradji-Aouat A (2005) Explicit FEA and constitutive modelling of damage and fracture in polycrystalline ice-simulations of ice loads on structures. Proceedings of 18th International Conference on Port and Ocean Engineering under Arctic Conditions.

Derradji-Aouat A, Sarzynski M, Cordes R (2015) Iceberg ice constitutive modeling and FEA validation. OTC Arctic Technology Conference.

Deshpande VS, Fleck NA (2000) Isotropic constitutive models for metallic foams. Journal of the Mechanics and Physics of Solids 48(6-7):1253-1283.

Drucker DC, Prager W (1952) Soil mechanics and plastic analysis or limit design. Quarterly of applied mathematics 10(2):157-165.

Gagnon R, Gammon P (1995) Triaxial experiments on iceberg and glacier ice. Journal of Glaciology 41(139):528-540.

Gagnon R, Derradji-Aouat A (2006) First results of numerical simulations of bergy bit collisions with the CCGS terry fox icebreaker. Proceedings of the 18th IAHR International Symposium on Ice, Sapporo, IAHR & AIRH, Japan.

Gagnon R (2007) Results of numerical simulations of growler impact tests. Cold Regions Science and Technology 49(3):206-214.

Gagnon R (2010) Numerical rendition of ice crushing. 20th IAHR International Symposium on Ice.

Gagnon R (2011) A numerical model of ice crushing using a foam analogue. Cold Regions Science and Technology 65(3):335-350.

Gagnon R, Wang J (2012) Numerical simulations of a tanker collision with a bergy bit incorporating hydrodynamics, a validated ice model and damage to the vessel. Cold Regions Science and Technology 81:26-35.

Golding N, Schulson EM, Renshaw CE (2010) Shear faulting and localized heating in ice: The influence of confinement. Acta Materialia 58(15):5043-5056.

Gratz E, Schulson E (1997) Brittle failure of columnar saline ice under triaxial compression. Journal of Geophysical Research: Solid Earth 102(B3):5091-5107.

Gupta V, Bergström JS (2002) A progressive damage model for failure by shear faulting in polycrystalline ice under biaxial compression. International Journal of Plasticity 18(4):507-530.

Han D, Lee H, Choung J, Kim H, Daley C (2017) Cone ice crushing tests and simulations associated with various yield and fracture criteria. Ships and Offshore Structures 12(sup1):302-311.

Iliescu D, Schulson EM (2004) The brittle compressive failure of fresh-water columnar ice loaded biaxially. Acta Materialia 52(20):5723-5735.

Ince ST, Kumar A, Paik JK (2017) A new constitutive equation on ice materials. Ships and Offshore Structures 12(5):610-623.

Ince ST, Kumar A, Park DK, Paik JK (2017) An advanced technology for structural crashworthiness analysis of a ship colliding with an ice-ridge: Numerical modelling and experiments. International Journal of Impact Engineering 110:112-122.

Jones SJ (2007) A review of the strength of iceberg and other freshwater ice and the effect of temperature. Cold Regions Science and Technology 47(3):256-262.

Jordaan IJ, Matskevitch DG, Meglis IL (1999) Disintegration of ice under fast compressive loading. International journal of fracture 97(1):279-300.

Jordaan IJ (2001) Mechanics of ice–structure interaction. Engineering Fracture Mechanics 68(17-18):1923-1960.

Kim H, Kedward K (1999) Experimental and numerical analysis correlation of hail ice impacting composite structures. 40th Structures, Structural Dynamics, and Materials Conference and Exhibit.

Kim H, Kedward KT (2000) Modeling hail ice impacts and predicting impact damage initiation in composite structures. AIAA journal 38(7):1278-1288.

Kim H (2015) Simulation of compressive 'cone-shaped' ice specimen experiments using LS-DYNA. Proceedings of the 13th International LS-DYNA Users Conference Dearborn, MI, USA.

Kim H, Daley C, Colbourne B (2015) A numerical model for ice crushing on concave surfaces. Ocean Engineering 106:289-297.

Kim H, Quinton B (2016) Evaluation of moving ice loads on an elastic plate. Marine Structures 50:127-142.

Kim J-H, Kim Y (2019) Numerical simulation of concrete abrasion induced by unbreakable ice floes. International Journal of Naval Architecture and Ocean Engineering 11(1):59-69.

Liu Z, Amdahl J, Løset S (2011) Plasticity based material modelling of ice and its application to ship–iceberg impacts. Cold Regions Science and Technology 65(3):326-334.

Michel B, Toussaint N (1977) Mechanisms and theory of indentation of ice plates. Journal of Glaciology 19(81):285-300.

Mokhtari M, Kim E, Amdahl J (2022) Pressure-dependent plasticity models with convex yield loci for explicit ice crushing simulations. Marine Structures 84:103233.

O'Rourke BJ, Jordaan IJ, Taylor RS, Gürtner A (2016) Experimental investigation of oscillation of loads in ice high-pressure zones, part 1: Single indentor system. Cold Regions Science and Technology 124:25-39.

Obisesan A, Sriramula S (2018) Efficient response modelling for performance characterisation and risk assessment of ship-iceberg collisions. Applied Ocean Research 74:127-141.

Price A, Quinton BW, Veitch B (2021) Shared-energy prediction model for ship-ice interactions. SNAME Maritime Convention.

Sain T, Narasimhan R (2011) Constitutive modeling of ice in the high strain rate regime. International Journal of Solids and Structures 48(5):817-827.

Sammonds P, Murrell S, Rist M (1998) Fracture of multiyear sea ice. Journal of Geophysical Research: Oceans 103(C10):21795-21815.

Schulson EM (1990) The brittle compressive fracture of ice. Acta Metallurgica et Materialia 38(10):1963-1976.

Schulson EM, Gratz ET (1999) The brittle compressive failure of orthotropic ice under triaxial loading. Acta Materialia 47(3):745-755.

Schulson EM (2001) Brittle failure of ice. Engineering Fracture Mechanics 68(17):1839-1887.

Shazly M, Prakash V, Lerch BA (2009) High strain-rate behavior of ice under uniaxial compression. International Journal of Solids and Structures 46(6):1499-1515.

Sinha NK (1978a) Rheology of columnar-grained ice. Experimental Mechanics 18(12):464-470.

Sinha NK (1978b) Short-term rheology of polycrystalline ice. Journal of Glaciology 21(85):457-474.

Sinha NK (1983) Creep model of ice for monotonically increasing stress. Cold Regions Science and Technology 8(1):25-33.

Sinha NK (1988) Crack-enhanced creep in polycrystalline material: strain-rate sensitive strength and deformation of ice. Journal of materials science 23(12):4415-4428.

Snyder SA, Schulson EM, Renshaw CE (2016) Effects of pre-strain on the ductile-to-brittle transition of ice. Acta Materialia 108:110-127.

Taylor RS. 2010. Analysis of scale effect in compressive ice failure and implications for design Memorial University of Newfoundland.

Timco GW, Frederking RMW (1986) Confined compression tests: Outlining the failure envelope of columnar sea ice. Cold Regions Science and Technology 12(1):13-28.

Tsai SW, Wu EM (1971) A general theory of strength for anisotropic materials. Journal of composite materials 5(1):58-80.

Wang B, Yu H-C, Basu R (2008) Ship and ice collision modeling and strength evaluation of LNG ship structure. International Conference on Offshore Mechanics and Arctic Engineering.

Weiss J, Schulson EM (1995) The failure of fresh-water granular ice under multiaxial compressive loading. Acta Metallurgica et Materialia 43(6):2303-2315.

Xiao J, Jordaan I (1996) Application of damage mechanics to ice failure in compression. Cold Regions Science and Technology 24(3):305-322.

Xiao J. 1997. Damage and fracture of brittle viscoelastic solids with application to ice load models Memorial University of Newfoundland.